Analysis of Fatigue Behavior of High-Density Polyethylene Based on Dynamic Viscoelastic Measurements during the Fatigue Process

ATSUSHI TAKAHARA, KENJI YAMADA, TISATO KAJIYAMA, and MOTOWO TAKAYANAGI, *Department of Applied Chemistry, Faculty of Engineering, Kyushu University 36, Hakozaki, Higashi-ku, Fukuoka, 812 Japan*

Synopsis

The fatigue behavior of high-density polyethylene was studied by measuring the variation in the dynamic viscoelasticity during the fatigue process. Brittle failure was observed under the conditions of small imposed strain amplitude, low ambient temperature, and large heat transfer coefficient to the surroundings. Ductile failure was observed under the conditions of large imposed strain amplitude, high ambient temperature, and small heat transfer coefficient to the surroundings. In the case of brittle failure, absolute value of dynamic complex modulus, $|E^*|$, showed maximum and phase difference, δ, did minimum on approaching the point of failure. In the case of ductile failure, $|E^*|$ decreased and δ increased monotonously from the start of the fatigue testing. The effect of environmental conditions on fatigue behavior was elucidated in terms of the heat transfer coefficient to the surroundings. As both forced convection of air and water enlarge the heat transfer coefficient, temperature rise of the specimen hardly occured and brittle failure took place preferentially. The coefficient, χ, was introduced to express the ratio of the actual generated heat to the hysteresis loss. With increase of the magnitude of the strain amplitude, the nonlinear viscoelastic behavior appeared and χ became smaller. A positive correlation between χ and lifetime was found. As the heat generation rate does not strongly affect lifetime, it was concluded that the hysteresis loss with low efficiency of heat generation would contribute to the fatigue failure. The relationship between average hysteresis loss and lifetime was proposed. The total hysteresis loss up to fatigue failure is constant, being independent of ambient temperature and imposed strain amplitude. The cumulative damage theory of fatigue failure was proposed based on hysteresis loss.

INTRODUCTION

The fatigue behavior of polymeric engineering materials has received growing attention in recent years. This is because the elucidation of fatigue mechanism is one of the most important problem with respect to the security of engineering materials. Two types of failure, i.e., brittle and ductile, have been generally reported.[1-3] These fatigue behaviors depend considerably on the fatigue test conditions such as ambient temperature,[1-3] environmental media,[4] imposed stress and strain amplitudes,[1-3] sample shape,[5] and testing frequency.[6] These testing conditions are closely related to the viscoelastic properties of polymeric materials. An increase of ambient temperature reduces fatigue lifetime and fatigue limit, owing to activation of the thermal molecular motion of polymer chains. The temperature dependence of fatigue lifetime has been described by Zhurkov's model of static failure.[7,8] Application of this theory, however, is limited only to the polymeric fibers with high degrees of crystallinity. An increase of imposed stress or strain amplitude also reduces fatigue lifetime,

Journal of Applied Polymer Science, Vol. 26, 1085–1104 (1981)

0021-8995/81/041085-20$02.00

probably because of activation of scission of polymer chains[9] or plastic deformation.[10] The environmental media with large heat transfer coefficient and high heat capacity contributes to an increase in fatigue lifetime, because heat generated due to the damping properties of the specimen is transferred to these media.[4] The surface active agent reduces the fatigue lifetime,[11] because the surface energy of the propagating crack is decreased by its adsorption to the crack surface. The sample shape also influences the heat transfer rate to the surroundings. The large ratio of the surface area to the volume of the specimen is effective for the heat transfer to the surroundings.[12]

The elucidation of fatigue mechanism was based on Wholer's curve method,[1-3,13] which has been initially applied to fatigue of metals. More theoretical methods have been proposed on the basis of the criterion that the total hysteresis energy dissipated up to fatigue failure was always constant in the case of fatigue of metals.[14] The application of this method to polymeric materials was performed by Higuchi and Imai[15] based on the temperature rise of the specimen during the fatigue process, and also by the authors of this article with consideration of viscoelastic energy loss.[16-18]

In this study, the effects of environmental conditions on the fatigue behavior of high-density polyethylene are discussed on the basis of the variation in dynamic viscoelasticity during the fatigue process under various environmental media and ambient temperatures. Also, the fatigue lifetime is qualitatively discussed based on its nonlinear viscoelasticity; and the quantitative relationship between hysteresis loss and fatigue lifetime is proposed.

EXPERIMENTAL

Sample Preparation for Fatigue Test

The sample used was high-density polyethylene (Novatec ET010, Mitsubishi Kasei Co., Ltd., melt index = 1.0). High-density polyethylene was compression molded into a dumbbell-shaped mold, with the dimensions shown in Figure 1, in a laboratory press at a temperature of 430 K for 40 min and quenched by plunging into ice water. The testing pieces were annealed at 393 K for 3 hr.

Fatigue Test

A tension–compression-type fatigue tester was designed in order to continuously record both absolute value of the dynamic complex modulus, $|E^*|$, and the phase difference, δ, between stress and strain under constant strain amplitude. Figure 2 shows the block diagram of the measuring system of the fatigue tester. The stress and strain signals were detected as electric signals, and these

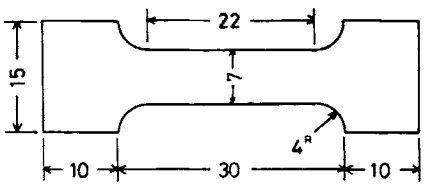

Fig. 1. Dimension of 5-mm thick specimen used in fatigue test.

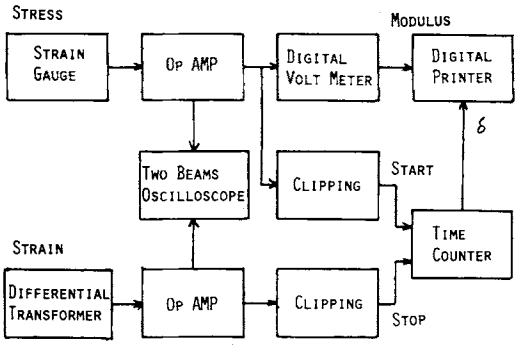

Fig. 2. Block diagram of measuring system of fatigue tester.

signals were amplified by an I.C. preamplifier. The absolute value of the dynamic complex modulus was estimated by dividing the stress value by the magnitude of strain amplitude which has been measured before fatigue testing. The phase difference, δ, was evaluated by measuring the time lag between stress and strain signals with a time counter. As the applied strain amplitude is large, nonlinear viscoelastic behavior was observed. In the nonlinear viscoelastic behavior, phase difference, δ, varies as a function of the angle at which it is measured.[19–21] As this equipment does not allow determination of δ as a function of the angle during the cycle, the time lag was measured at zero voltage for each signal. As the hysteresis loop is sufficiently elliptical, hysteresis loss (hysteresis loop area) h was calculated from the following equation:

$$h = \pi \epsilon_0 \sigma \sin\delta$$

where ϵ_0 and σ are the magnitudes of strain and stress amplitudes, respectively. These data were recorded automatically using a digital printer. The details of the testing apparatus are shown elsewhere.[16,18] The testing frequency was 6.91 Hz. The fatigue test was carried out under natural convection or forced convection of air, or in water. Under natural convection, ambient temperature was controlled by an air bath equipped with a thermocontroller. Under forced convection of air, a blower with an air-blowing velocity of 2.7 $m^3\ min^{-1}$ was set near the specimen to remove heat generated under cyclic straining. Also, the fatigue test was performed soaking the specimen in a water bath at temperatures of 285 and 315 K.

Observation of Fatigue Fracture Surface

A scanning electron microscope (SEM, Hitachi S-430) was used for morphological observations of the fatigue fracture surface of the test specimen.

Measurement of Heat of Fusion

The heat of fusion for the original specimen and those subjected to cyclic fatigue were measured with a differential scanning calorimeter, UNIX (Rigaku Denki Co., Ltd.) at a heating rate of 10 K min^{-1}. The standard materials to calculate heat quantity were indium (In) and tin (Sn).

RESULTS AND DISCUSSION

S–N Curve

Figure 3 shows the *S–N* curves for various ambient temperatures and environmental media, respectively. The ordinate and abscissa in Figure 3 are the initial stress amplitude and the logarithmic lifetime, respectively. Under natural convection at the ambient temperatures of 295, 320, and 340 K [Fig. 3(a)], the fatigue fracture surface of the specimen shows smoothness characteristics of brittle failure, and the specimen temperature increases slightly at small stress amplitude. On the other hand, at large stress amplitude, the specimen temperature increases drastically and a small amount of plastic flow was observed on the fatigue fracture surface of the specimen. Figure 4 shows the scanning electron photomicrographs for the fatigue fracture surface of the specimen tested under forced convection of air at the ambient temperature of 292 K and the imposed strain amplitudes of 0.80 and 1.82%, respectively. The fatigue fracture surface subjected to the small imposed strain amplitude [Fig. 4(a)] is smoother than those subjected to the large imposed strain amplitude [Fig. 4(b)]. The

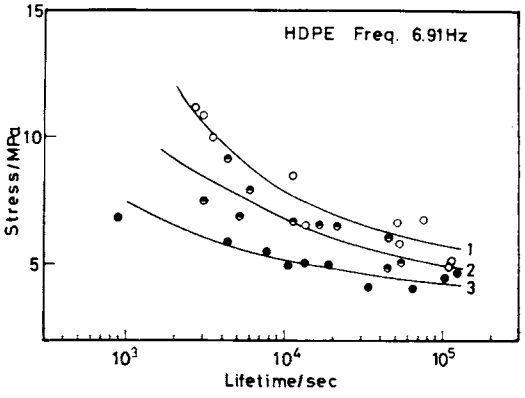

(a)

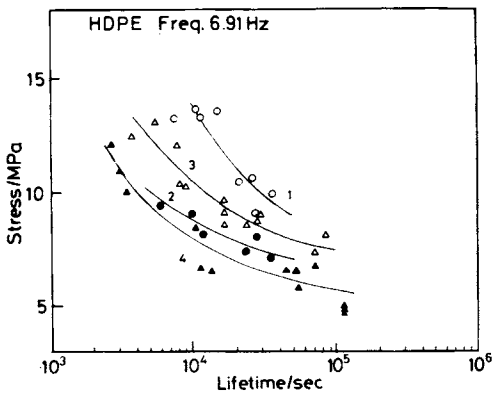

(b)

Fig. 3. *S–N* curves for (a) various ambient temperatures under normal convection, (b) various environmental media. HDPE frequency = 6.91 Hz. For (a), (1) ○, 295 K; (2) ◒, 320 K; (3) ●, 340 K. For (b), (1) ○, 285 K in H_2O; (2) ●, 315 K in H_2O; (3) △, 292 K under forced convection; (4) ▲, 295 K under natural convection.

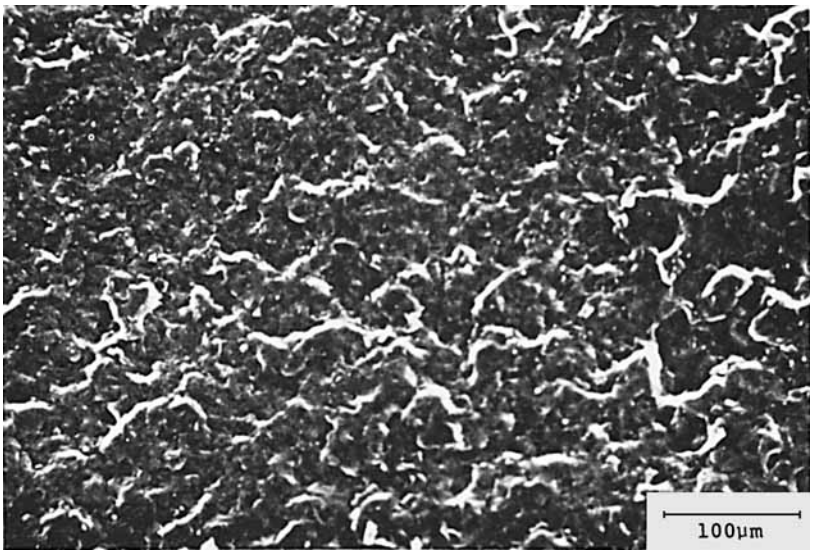

(a)

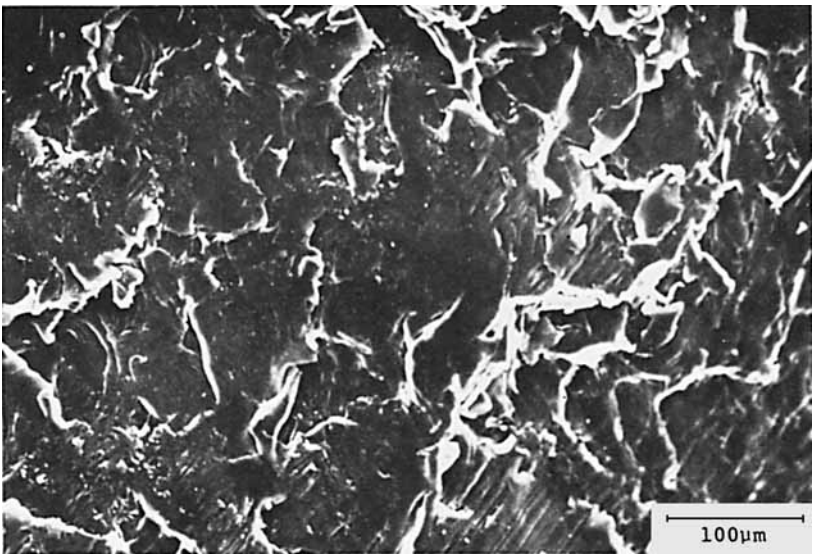

(b)

Fig. 4. Scanning electron photomicrographs of fatigue fracture surface of high-density polyethylene fractured under ambient temperature of 292 K under forced air convection at (a) strain amplitude of 0.80% and lifetime of 84,000 sec, (b) strain amplitude of 1.82% and lifetime of 3,900 sec.

rough surface indicates that there is considerable contribution of ductility; in other words, degree of plastic deformation during the crack propagation process. The increase in the ambient temperature makes the lifetime shorten at the same stress amplitude. The effect of the environmental condition on fatigue lifetime is apparent in comparing the curves (1–4) in Figure 3(b). Just forced convection of air and soaking of the specimen in water make the heat transfer rate to the surroundings increase, it is apparent that the effective removal of generated heat under cyclic straining prolonged the fatigue lifetime.

Variation of Dynamic Viscoelasticity during Fatigue Process

Figure 5 shows the variation in absolute value of the dynamic complex modulus, $|E^*|$, phase difference, δ, and hysteresis loss, h, during the fatigue process under natural convection of air at the ambient temperature of 295 K as a function of strain amplitudes. The decrease of $|E^*|$ and the increase of δ are due to the temperature rise of the specimen toward attainment of the thermally steady state. The initial decrease of $|E^*|$ and the increase of δ became more distinctive with an increase in imposed strain amplitude. At relatively small imposed strain amplitudes of 0.94, 1.03, and 1.49% (curves 1–3, Fig. 5), both $|E^*|$ and δ became roughly constant after their initial variation; this is probably due to the attain-

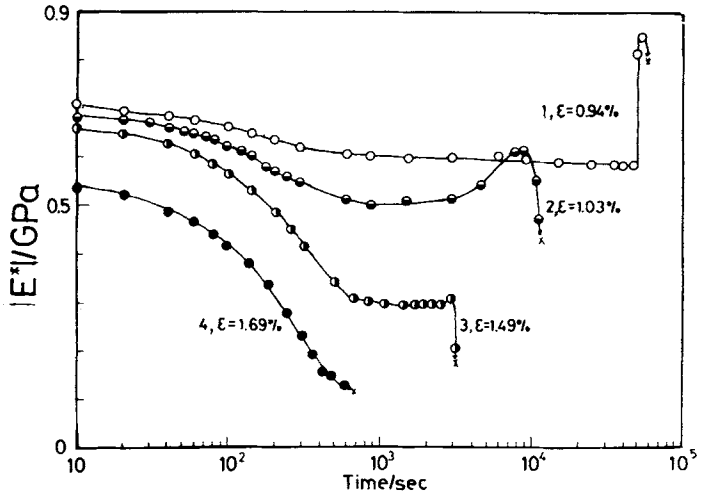

(a)

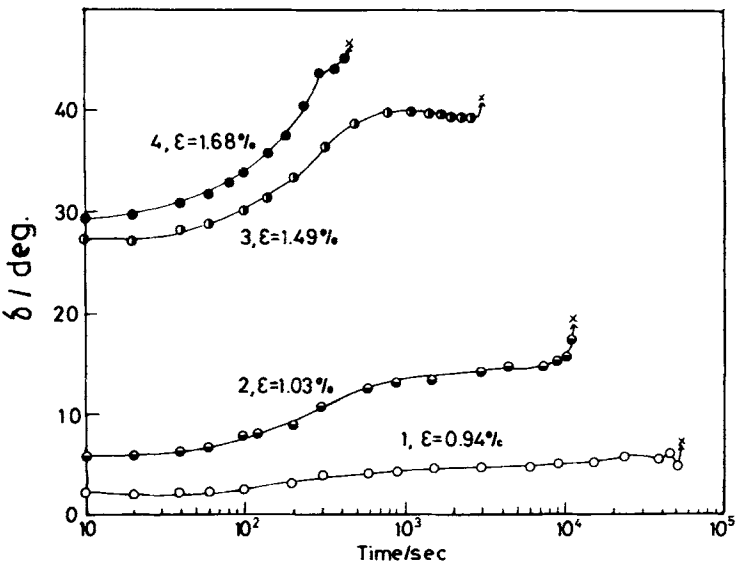

(b)

Fig. 5. Variation of (a) $|E^*|$; (b) δ; (c) h during fatigue process at ambient temperature of 295 K under natural convection as function of strain amplitudes. Frequency is 6.91 Hz.

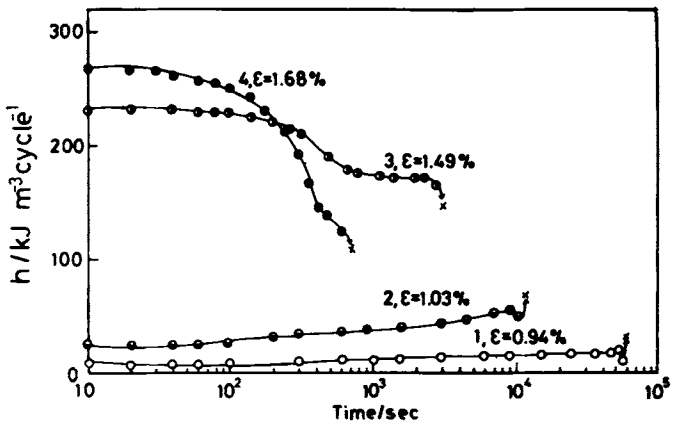

(c)

Fig. 5. (*Continued from previous page*)

ment of thermally steady state. At a large imposed strain amplitude of 1.69% (curve 4 in Fig. 5), $|E^*|$ decreased and δ increased monotonously from the start of the fatigue testing. In this case, rupture took place during the rising process of the specimen temperature. This fatigue behavior resembles thermal failure of plasticized poly(vinyl chloride) in which the specimen temperature reaches the glass transition temperature and thermal softening ultimately occurs.[16–18] In the case of small imposed strain amplitudes of 0.94 and 1.03% (curves 1 and 2, Fig. 5), the viscoelastic behavior characteristic of brittle failure can be observed, that is, the increase of $|E^*|$ takes place followed by the rapid growth of cracks leading to rupture. The typical behavior of brittle failure like this has been observed in plasticized poly(vinyl chloride),[16–18] segmented poly(urethaneureas),[22] and dog compact bone.[23,24] The maximum of $|E^*|$ and the minimum of δ in the vicinity of rupture became more apparent in the case of smaller imposed strain amplitudes (curves 1 and 2 in Fig. 5), and this tendency disappeared with an increase in the strain amplitude (curve 4, Fig. 5). The maximum of $|E^*|$ and the minimum of δ indicate that the contribution of elastic term to viscoelastic properties increases at the final stage of fatigue and that this may be due to the preferential orientation of polymer chains in the direction of the cyclic straining.

Figure 6 shows the variation of $|E^*|$, δ, and h during the fatigue process at the ambient temperature of 292 K under forced convection of air as a function of imposed strain amplitudes. The slight variation of $|E^*|$ and δ at an initial stage of the fatigue process suggests the effective removal of generated heat from the specimen and that the specimen temperature hardly increases. The characteristic feature of brittle failure with respect to $|E^*|$ and δ was observed even at a relatively large strain amplitude (curve 3, Fig. 6), in comparison to the case of natural convection. At a large imposed strain amplitude of 1.93% (curve 4, Fig. 6), $|E^*|$ did not show maximum on approaching the point of failure, but decreased abruptly at the point of failure. The imposed strain amplitude of 1.93% under forced convection of air would correspond to the intermediate conditions between brittle and ductile failures.

The remarkable effect of the removal of generated heat was also observed when

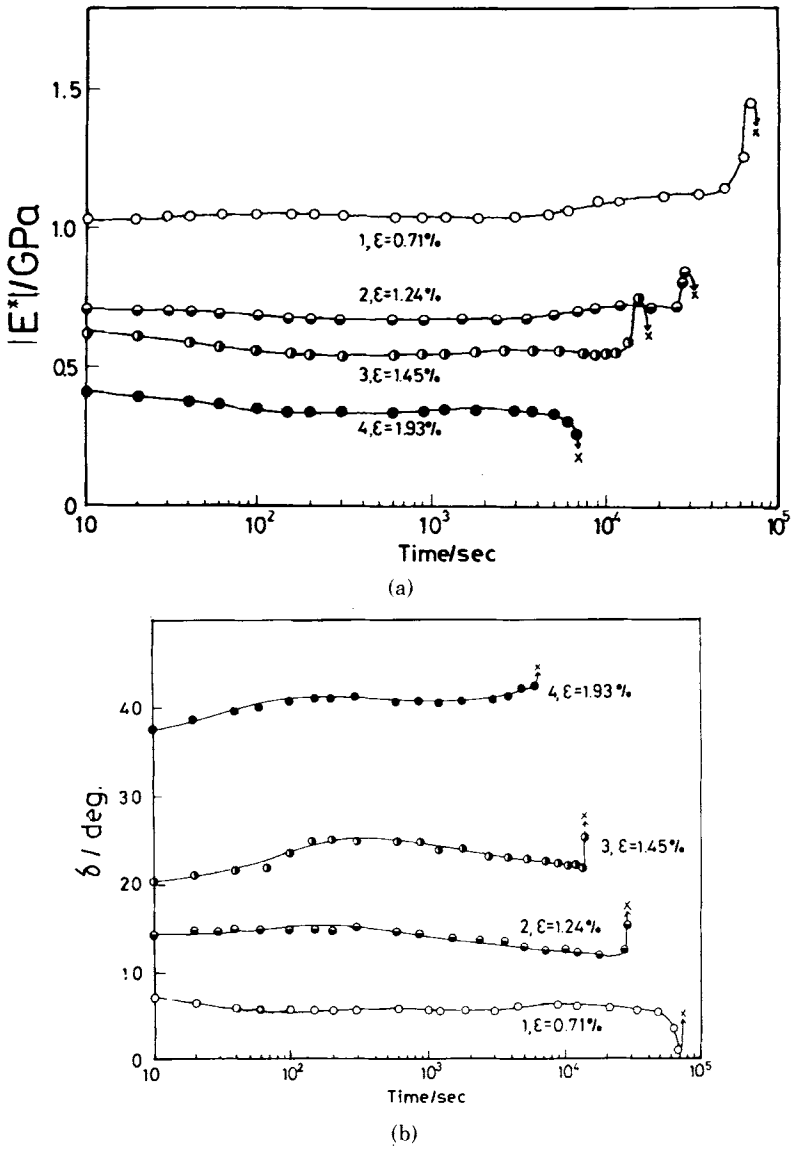

Fig. 6. Variation of (a) $|E^*|$; (b) δ; (c) h during fatigue process at ambient temperature of 292 K under forced convection of air as function of strain amplitudes. Frequency is 6.91 Hz.

the specimen was fatigued in water. Figure 7 shows the variation of $|E^*|$, δ, and h during the fatigue process in water at the ambient temperature of 285 K as a function of imposed strain amplitudes. The characteristic feature of brittle failure was observed even at a larger strain amplitude than that under natural convection of air at 295 K.

Figure 8 shows the variation of $|E^*|$, δ, and h during the fatigue process at the ambient temperature of 340 K, under natural convection as a function of imposed strain amplitudes. The characteristic feature of brittle failure was observed only at the small imposed strain amplitude of 0.82% (curve 1 in Fig. 8). Intermediate

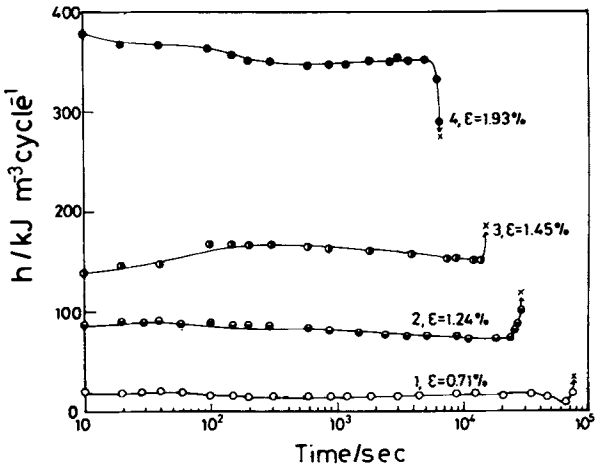

(c)

Fig. 6. (*Continued from previous page*)

behavior between brittle and ductile failures was observed at relatively small imposed strain amplitudes (curves 2–4, Fig. 8).

From the results obtained under various fatigue conditions, it may be concluded that the conditions of lower ambient temperature, smaller imposed strain amplitude, and greater heat transfer rate to the surroundings increase the contribution of brittle failure to fatigue behavior. The characteristic viscoelastic behavior of brittle failure is the appearance of the maximum of absolute value of the dynamic complex modulus, $|E^*|$, and the minimum of phase difference, δ, on approaching the point of failure. Also, in the case of brittle failure, the specimen temperature increases slightly.

Effect of Environmental Media on Fatigue Failure

The effect of environmental media on fatigue behavior can be described in terms of the heat generation rate of the specimen, and the heat transfer rate to the surroundings.[16,25] The heat generation rate of the specimen due to the damping property of the specimen is represented by eq. (1):

$$Q_+ = \chi f \cdot h(T_s) \tag{1}$$

where f and $h(T_s)$ are the frequency and hysteresis loss at the specimen temperature, T_s, respectively. The correction factor, χ, which shows the ratio of the actual heat generation rate to the apparent energy loss (hysteresis loss) per a unit time, must be introduced to correct the actual heat generation rate. The heat transfer rate to the surroundings is represented by eq. (2):

$$Q_- = \kappa(T_s - T_0) = \kappa\theta \tag{2}$$

where κ, T_0, and θ are the heat transfer coefficient to the surroundings, the ambient temperature, and the degree of temperature rise of the specimen, respectively.

Equation (3) expresses the rate of the net temperature rise of the specimen during the fatigue process:

$$\frac{dT_s}{dt} = \frac{(Q_+ - Q_-)}{\rho c} \tag{3}$$

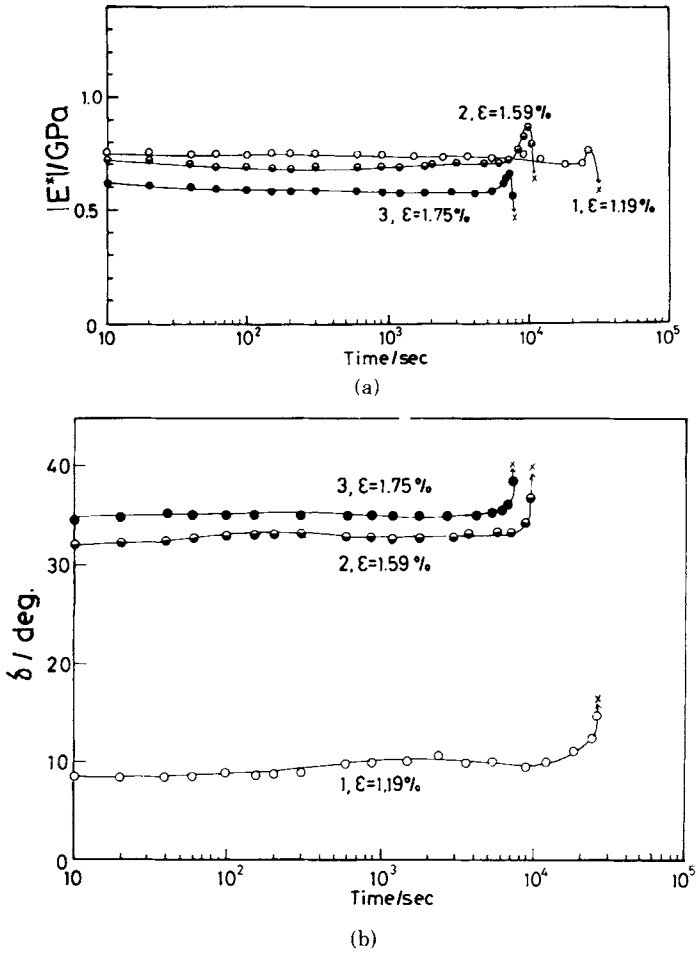

Fig. 7. Variation of (a) $|E^*|$; (b) δ; (c) h during fatigue process at ambient temperature 285 K in water as function of strain amplitudes. Frequency is 6.91 Hz.

where ρ and c are the density and specific heat of the specimen. Figure 9 shows the temperature rise of the specimen, θ, increases at the initial stage of fatigue process and attains thermally steady-state temperature under the conditions of an ambient temperature of 295 K, a strain amplitude of 0.93 %, and of natural convection. The variation in absolute value of the dynamic complex modulus, $|E^*|$, and hysteresis loss, h, at the initial stage of the fatigue process could be observed corresponding to the temperature rise of the specimen.

If the specimen temperature continues to rise, eq. (4) should hold:

$$Q_+ \geqq Q_-$$
$$\chi f \cdot h(T_s) \geqq \kappa(T_s - T_0) \tag{4}$$

where an equality means thermally steady state. Figure 10 illustrates the relationship between the heat generation rate of the specimen, Q_+, and the heat transfer rate to the surroundings, Q_-. The curve of the heat generation rate, Q_+, shows the peak corresponding to the absorption temperature region of the dynamic loss modulus, E''. As the magnitude of the heat transfer coefficient,

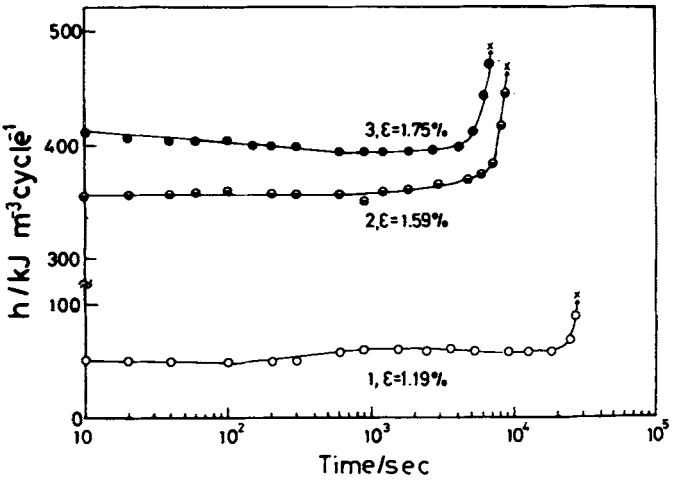

(c)

Fig. 7. (*Continued from previous page*)

κ, to the surroundings is proportional to the 0.8th power of volume velocity of the environmental media,[12] the fatigue conditions under forced convection of air makes the magnitude of κ increase. Also, an increase in the heat transfer coefficient was brought about by the large heat capacity of the environmental media such as water. Since κ is the slope of the Q_- line in Figure 10, an increase in the magnitude of κ results in lowering of the steady-state temperature as shown by "A." Therefore, it is apparent that characteristics of brittle failure become more prominent as represented by the tendency for of $|E^*|$ to decrease and by the increase of δ at the initial stage of the fatigue process, which scarcely occurred even at large strain amplitude; also, the maximum of $|E^*|$ and the minimum of δ on approaching the point of failure were observed even at large strain amplitude.

Also, this model of fatigue failure well elucidates the effects of ambient temperature and strain amplitude. The increase of ambient temperature and strain amplitude make the thermally steady-state temperature higher, so the characteristics of brittle failure becomes less prominent.

Qualitative Analysis of Fatigue Behavior Based on Nonlinear Viscoelasticity

As shown in the previous section, for thermally steady-state conditions under cyclic straining, eq. (5) holds:

$$\chi f \cdot h(T_{ss}) = \kappa(T_{ss} - T_0) \tag{5}$$

where T_{ss} is the specimen temperature at thermally steady state. The value of T_{ss} was evaluated directly by measuring the surface temperature of the specimen as a function of time at a given ambient temperature and imposed strain amplitude, as shown in Figure 9. The amount of temperature rise, θ_s, at the thermally steady state is expressed by eq. (6):

$$\theta_s = T_{ss} - T_0 = \chi f \cdot h(T_{ss})/\kappa \tag{6}$$

Figure 11 shows variation of θ_s with the square of the strain amplitude, ϵ^2, as a

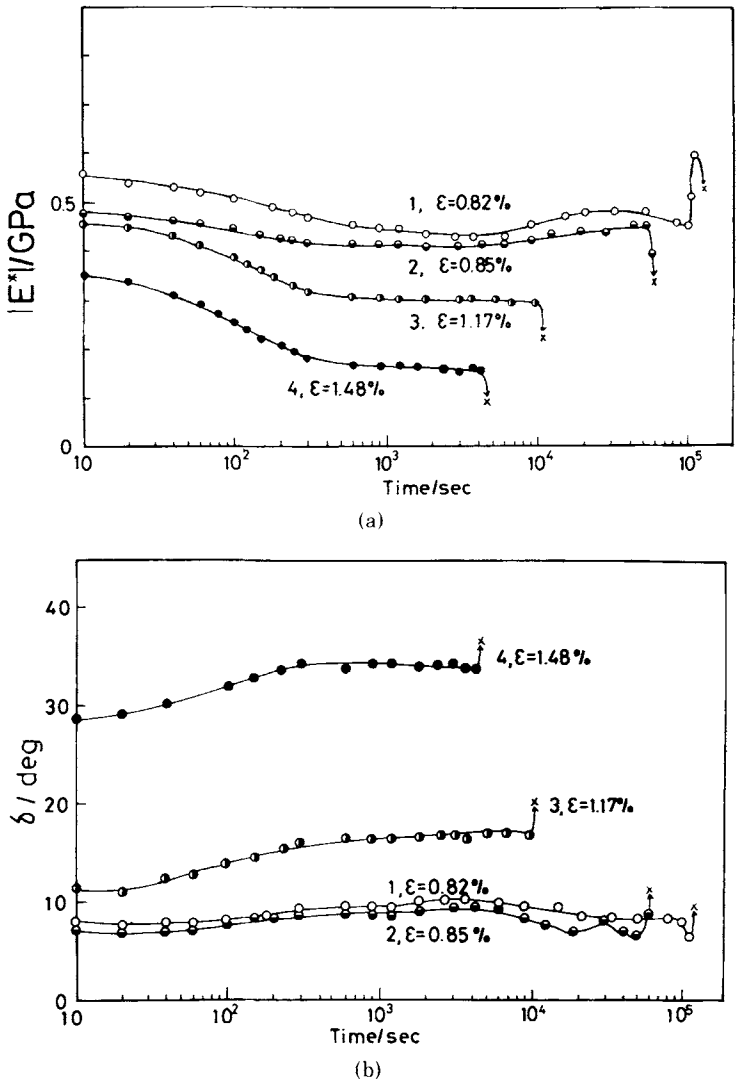

Fig. 8. Variation of (a) $|E^*|$; (b) δ; (c) h during fatigue process at ambient temperature of 340 K under natural convection as function of strain amplitudes. Frequency is 6.91 Hz.

function of ambient temperatures under natural convection. The amount of temperature rise at thermally steady state increases with the strain amplitude. In the linear viscoelastic region, the mechanical phase difference, δ, should not depend on the magnitude of the imposed strain amplitude at a steady-state temperature, and χ equals unity. Figure 12 shows the variation of $|E^*|$ and δ with imposed strain amplitude at the specimen temperature of 295 K. In the temperature range studied, it seems reasonable to consider that the nonlinear viscoelastic property[26] mainly contributes to and increase of δ and to a decrease in $|E^*|$ with strain amplitude. However, in these strain amplitudes, the shape of the stress signal was not distorted.

As the magnitude of phase difference, δ, increases with an increase in strain amplitude, it is supposed that the magnitude of χ decreases under the conditions

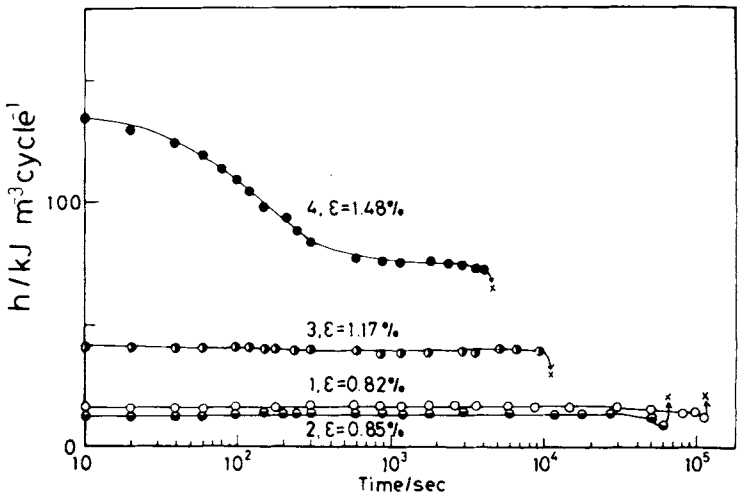

(c)

Fig. 8. (*Continued from previous page*)

that the magnitude of heat transfer coefficient, κ, does not change with the strain amplitude. On the basis of the nonlinear modulus obtained at steady-state temperature, the magnitude of χ/κ can be evaluated from eq. (7):

$$\chi/\kappa = \theta_s/[f \cdot h(T_{ss})] \tag{7}$$

Figure 13 shows the variation in χ/κ with strain amplitude, ϵ, at various ambient temperatures under natural convection. Figure 13 tells us that the magnitude of χ/κ decreases with an increase in the strain amplitude. This fact suggests that the efficiency of the heat generation rate to the total apparent energy loss (hysteresis loss) per unit time decreases with an increase in strain amplitude, assuming the independent magnitude of κ of strain amplitude. This behavior could be closely related to the nonlinear viscoelastic response to the dynamic strain amplitude or the change of structural implications. Figure 14 shows the variation

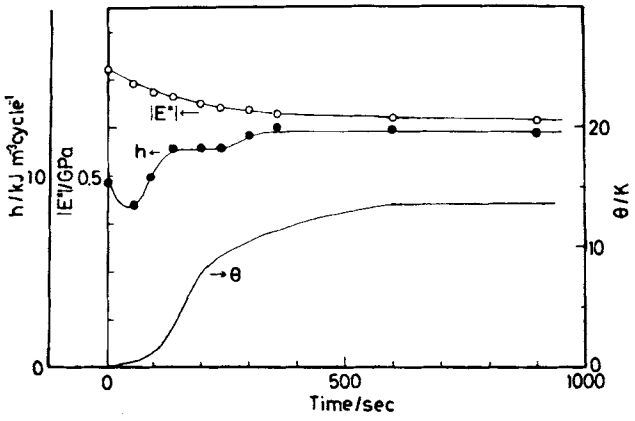

Fig. 9. Variation of $|E^*|$, h, and temperature rise of specimen, θ, during fatigue process under conditions of strain amplitude of 0.93% and ambient temperature of 295 K under natural convection.

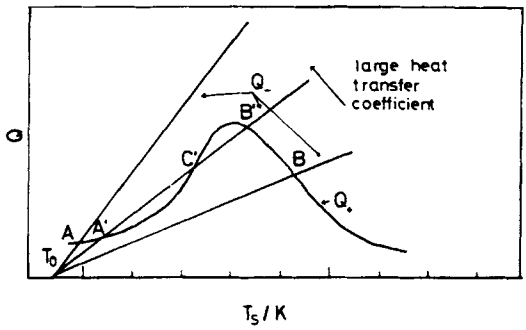

Fig. 10. Variation of heat generation rate of specimen, Q_+ and heat transfer rate to surroundings, Q_-, with specimen temperature, T_s as function of heat transfer coefficient.

of χ/κ with lifetime, t_f, for various ambient temperatures under natural convection. Data obtained at different ambient temperatures give a single curve, though the experimental values are slightly scattered. The magnitude of χ/κ

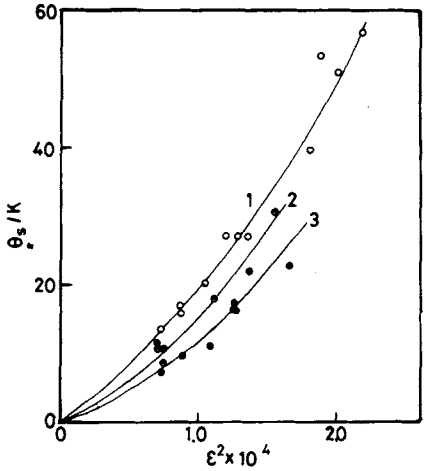

Fig. 11. Variation of specimen temperature rise, θ_s, at thermally steady state with square of strain amplitude, ϵ^2, for various ambient temperatures under natural convection. (1) ○, 295 K; (2) ⊖, 320 K; (3) ●, 340 K.

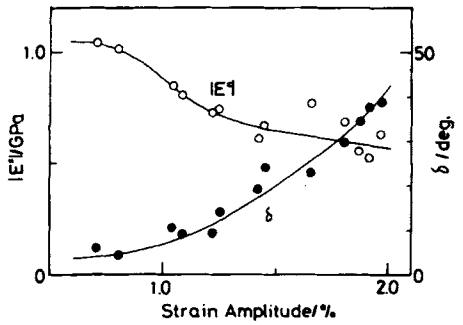

Fig. 12. Variation of absolute value of dynamic complex modulus, $|E^*|$, and phase difference, δ, with dynamic strain amplitude at specimen temperature of 295 K.

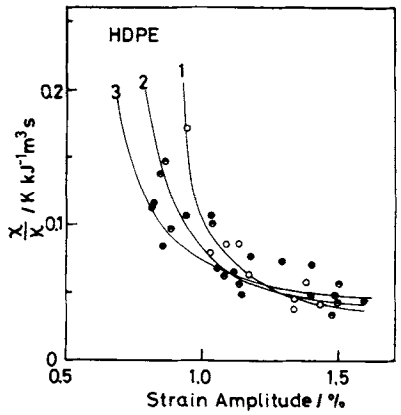

Fig. 13. Variation of χ/κ with strain amplitude for various ambient temperatures under natural convection. (1) ○, 295 K; (2) ⊖, 320 K; (3) ● 340 K.

is smaller in the shorter lifetime range. Tauchert[27] and Tauchert and Afzel[28] reported that the total hysteresis energy of some metals or polymeric materials did not reappear as heat, but some fraction of it might be consumed by internal energy changes due to the conformational change of the molecular chains. The energy loss (hysteresis loss) which does not accompany effective heat generation may be associated with fatigue damage in relation to the structural change leading to fatigue failure. Table I shows the magnitudes of heat of fusion after the fatigue process under various conditions. The samples for DSC measurement of heat of fusion were cut out apart from the fracture surface, because the region near the fracture surface is plastically deformed. As annealing temperature of the specimens prior to fatigue tests is higher than the highest temperature attained at steady state under cyclic fatigue, there are no influence of temperature rise on the magnitude of heat of fusion. The magnitude of heat of fusion of fatigued specimen is greater than that of the original sample. This fact may suggest that the energy loss (hysteresis loss), except heat generation, contributes to the increase in the degree of crystallinity.

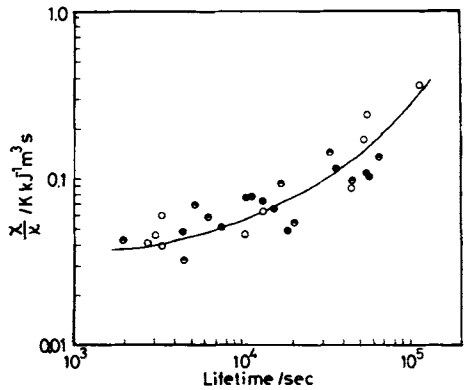

Fig. 14. Variation of χ/κ with lifetime, t_f, for various ambient temperatures under natural convection. ○, 295 K, ⊖, 320 K; ●, 340 K. Frequency is 6.91 Hz.

TABLE I
Variation of Heat of Fusion after Fatigue Process

T_0/K	t_f/sec	ΔH_f/cal g^{-1}
295	111,000	44.09
295	111,200	47.14
340	4,500	45.29
340	7,500	48.53
340	840	47.93
340	10,500	45.65
340	15,600	49.96
340	36,000	45.95
340	107,800	49.72
	original sample	42.38

Hysteresis Loss Related to Lifetime

The hysteresis loss (energy loss) for viscoelastic materials per unit time and unit volume under cyclic straining is given by eq. (8):

$$H = \pi f \epsilon_0 \sigma \cdot \sin\delta = f \cdot h(T_s) \tag{8}$$

The average hysteresis loss (energy loss) per unit time and unit volume in the fatigue cycle, H_{av}, is expressed as follows:

$$H_{av} = \left(\int_0^{t_f} H \, dt \right) / t_f \tag{9}$$

Figure 15 shows the variation of average energy loss, H_{av}, with lifetime, t_f, for various ambient temperatures under natural convection. The magnitude of H_{av} is dependent on lifetime as represented by the following equation:

$$H_{av} \cdot t_f = C \tag{10}$$

Figure 15 and eq. (10) express that failure occurs when the hysteresis energy reaches a certain magnitude, C. Also, eq. (10) holds true under forced convection of air and in water. Equation (10) holds true under the condition that the magnitude of stress amplitude is larger than 4.5 MPa. The magnitude of C are 3.5×10^6 kJ m^{-3} under natural convection and 2.3×10^7 kJ m^{-3} under forced

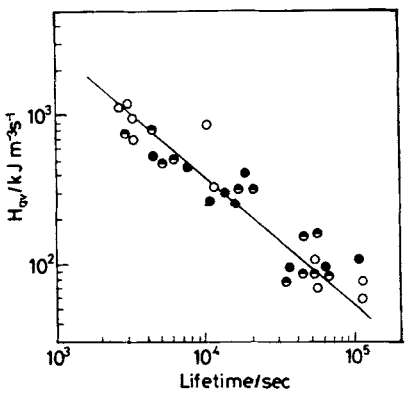

Fig. 15. Relationship between average hysteresis loss, H_{av}, and lifetime, t_f, for various ambient temperatures under natural convection. (1) ○, 295 K; (2) ◓, 320 K; (3) ●, 340 K. Frequency is 6.91 Hz.

convection of air and in water. These values are several hundred times larger than that of plasticized poly(vinyl chloride)[16–18] in the temperature range of from 295 to 325 K. The magnitude of C may indicate that high-density polyethylene is more fatigue resistant than plasticized poly(vinyl chloride). In the case of plasticized poly(vinyl chloride), the magnitude of C was dependent on ambient temperature as represented by an Arrehenius-type equation,[16–18] whereas in this case, C is independent of ambient temperatures. This is probably due to the fact that the mechanism of thermal molecular motion of high-density polyethylene is not strongly dependent on temperature in the temperature region studied here, which is sufficiently higher than primary relaxation temperature and lower than crystalline relaxation temperature.[29]

Effect of Actual Heat Generation on Fatigue Behavior

The product of χ/κ and average hysteresis loss, H_{av}, is a measure of the absolute value of actual generated heat; in other words, the temperature rise of the specimen. Figure 16 shows the relationship between $\chi \cdot \kappa^{-1} \cdot H_{av}$ and fatigue lifetime, t_f, for various ambient temperatures under natural convection. The fatigue lifetime decreased with an increase in the actual generated heat. The more gentle slope of Figure 16, compared to Figure 15, indicates that the fatigue lifetime is not strongly dependent on hysteresis loss. The hysteresis loss (energy loss) causes heat generation accompanying change of structural implications, such as formation of microvoids or frictional heat due to the movement of microvoids; but, in the nonlinear viscoelastic region, the total hysteresis loss does not effectively convert to heat. As shown in Figure 13, with the increase in strain amplitude, it appears that the hysteresis loss does not accompany effective heat generation. From the results obtained in this section and previous sections, it may be concluded that the hysteresis loss, up to fatigue failure, is an important factor for measurement of fatigue lifetime. The energy loss may partially expedite the structural change or the change in crystallinity and ultimately lead to fatigue failure.

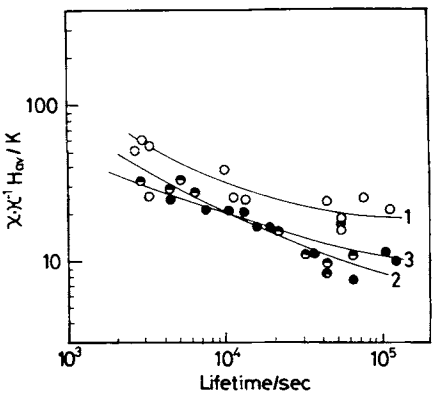

Fig. 16. Relationship between $\chi\kappa^{-1} \cdot H_{av}$ and lifetime, t_f, for various ambient temperatures under natural convection. (1) ○, 295 K; (2) ◓, 320 K; (3) ●, 340 K. Frequency is 6.91 Hz.

Cumulative Damage Theory Based on Hysteresis Loss

The concept that the fatigue damage is irreversible and cumulative has been applied to the fatigue study of metals. The most well-known law based on this concept is Miner's law[30] and a modified Miner's law has been proposed by several authors.[3,31] Miner's law was applied to the case of fatigue conditions with variation of stress amplitude during cyclic fatigue. When the stress amplitude of the ith process, σ_i, is applied to the test specimen for n_i cycles and also, the fatigue lifetime is N_i cycles at the stress amplitude of σ_i, the ultimate fatigue failure occurs when the summation of damage ratio, n_i/N_i reaches unity. That is:

$$\sum_{i=1}^{k} (n_i/N_i) = 1 \tag{11}$$

Prevorsek and Brooks applied this theory to the polymeric fibers based on crack-nucleation theory.[32] We applied this cumulative damage theory to bulk polyethylene based on the relationship between hysteresis loss and fatigue lifetime.

If the imposed strain amplitude and the ambient temperature are varied during the fatigue process, the summation of hysteresis loss, C_i, at the ith stage of the fatigue process (the ambient temperature = T_{0i}, the strain amplitude = ϵ_i, and fatigue time = t_i) is expressed as follows:

$$H_{av,i}t_i = C_i \tag{12}$$

where $H_{av,i}$ is an average hysteresis loss at the ith stage of the fatigue process. Then, the criterion for fatigue failure is proposed; that is, the ultimate fatigue failure occurs when the sum of hysteresis loss at each stage of the fatigue process reaches the effective hysteresis loss for fatigue failure, C, in eq. (10):

$$\sum_{i=1}^{k} H_{av,i}t_i = \sum_{i=1}^{k} C_i = C \tag{13}$$

Then eq. (13) is rewritten in terms of the summation of the damage ratio, C_i/C:

$$\sum_{i=1}^{k} (C_i/C) = 1 \tag{14}$$

Equation (14) is the modified Miner's law based on hysteresis loss including variation in the strain amplitude and the ambient temperature during the fatigue process. Table II tabulates the hysteresis loss, C_i, and the damage ratio, C_i/C, at the ith stage of the fatigue process under the conditions of the strain amplitude, ϵ_i, and the ambient temperature, $T_{0,i}$. It may be concluded that the fatigue damage is irreversible and cumulative, since the summation of the damage ratio, C_i/C, up to fatigue failure is around unity. Also, eqs. (12)–(14) hold under the conditions that the magnitude of stress amplitude is larger than 4.5 MP_a.

CONCLUSIONS

Two types of brittle and ductile failures were found in fatigue behavior of high-density polyethylene. Brittle failure occurred under the conditions of low ambient temperature, small imposed strain amplitude, and large heat transfer coefficients to the surroundings. The characteristic viscoelastic behavior of brittle failure is that the absolute value of the dynamic complex modulus, $|E^*|$,

TABLE II
Verification of Cumulative Damage Theory Based on Hysteresis Loss during Fatigue Process

No.	T_0/K	ϵ/%	$10^{-6}C_i$/kJ m^{-3}	C_i/C	$(\Sigma C_i)/C$
1	285	1.27	5.9	0.26	0.88
	285	1.67	14.3	0.62	
2	305	1.82	8.8	0.38	1.11
	290	1.70	16.7	0.73	
3	310	1.83	22.3	0.97	1.24
	287	1.04	6.2	0.27	
4	312	1.83	12.8	0.56	0.81
	289	1.01	5.8	0.25	
5	313	1.19	2.3	0.10	
	289	1.72	10.0	0.43	0.84
	289	0.98	7.9	0.31	
6	310	1.86	18.4	0.80	0.87
	289	1.04	1.5	0.07	
7	307	1.89	17.0	0.74	1.05
	287	1.25	7.3	0.31	
				average	0.97

shows a maximum and phase difference, δ, shows a minimum upon approaching the point of failure. On the other hand, ductile failure occurred under the conditions of high ambient temperature, large imposed strain amplitude, and small heat transfer coefficient to the surroundings. The characteristic viscoelastic behavior of ductile failure is that $|E^*|$ decreases and δ increases monotonously from the start of the fatigue testing. Under the intermediate conditions of ductile and brittle failures, $|E^*|$ and δ are almost constant up to fatigue failure, and $|E^*|$ decreases and δ increases at the point of failure.

The effect of environmental conditions on fatigue behavior was explained by the relationship between the heat generation rates of the specimen, depending on their damping property and the heat transfer rate to the surroundings. The heat transfer rate increased under forced convection of air or by soaking of the specimen in water. An increase in the heat transfer rate to the surroundings makes the thermal steady-state temperature lower and also, brittle failure preferentially occurred.

It was found out that the hysteresis loss contributes to the fatigue damage. The relationship between the average hysteresis loss, H_{av}, during the fatigue process and lifetime, t_f, has been derived:

$$H_{av} \cdot t_f = C$$

The total hysteresis loss up to fatigue failure, C, is constant, independent of ambient temperature and imposed strain amplitudes. From the measurements of specimen temperature and hysteresis loss at the thermally steady state, actual heat generation rate of the specimen was evaluated. The ratio of the actual generated heat to the apparent energy loss (hysteresis loss) decreased with the increase in strain amplitude. This fact suggests that with the increase in non-

linear viscoelastic behavior, the heat generation rate of the specimen was suppressed.

Based on the relationship between hysteresis loss and lifetime, a cumulative damage theory was proposed:

$$\sum_{i=1}^{k} H_{av,i} t_i = \sum_{i=1}^{k} C_i = C$$

where $H_{av,i}$ and C_i are average hysteresis loss and the total hysteresis loss at the ith stage of the fatigue process under the conditions of the ambient temperature of $T_{0,i}$ and the strain amplitude of ϵ_i, respectively.

References

1. H. H. Kausch, *Polymer Fracture*, Springer Verlag, Berlin, 1978, p. 220.
2. E. H. Andrews, *Fracture in Polymers*, Oliver & Boyd, Edinburg, 1969, p. 162.
3. R. W. Hertzberg, *Deformation and Fracture Mechanics of Engineering Materials*, Wiley, New York, 1976, p. 520.
4. S. B. Ratner and N. I. Barash, *Mekh, Polim.*, 1(1), 124 (1965).
5. M. N. Ridell, G. P. Koo, and J. L. O'Toole, *Polym. Eng. Sci.*, **6**, 363 (1966).
6. D. A. Opp, D. W. Skinner, and R. J. Wiktorek, *Polym. Eng. Sci.*, **9**, 121 (1969).
7. V. R. Regel and A. M. Leksovskii, *Int. J. Frac. Mech.*, **3**, 99 (1967).
8. V. P. Tamuzh, *Mekh, Polim.*, **5**, 907 (1969).
9. T. Nagamura, N. Kusumoto, and M. Takayanagi, *J. Polym. Sci., Polym. Phys. Ed.*, **11**, 2537 (1973).
10. K. C. Rusch and R. H. Beck, Jr., *J. Macromol. Sci. Phys., B*, **3**, 365 (1969).
11. S. Okuda and S. Nishina, *Proc. JSTM*, **9**, 109 (1966).
12. W. H. McAdams, *Heat Transmission*, 3rd ed., McGraw-Hill, New York, 1954.
13. J. H. Dillon, *Adv. Colloid. Sci.*, **3**, 229 (1951).
14. C. E. Feltner and J. D. Morrow, *Trans. ASME, Ser. D*, **83**, 15 (1961).
15. M. Higuchi and Y. Imai, *J. Appl. Polym. Sci.*, **14**, 2379 (1970).
16. A. Takahara, K. Yamada, T. Kajiyama, and M. Takayanagi, *J. Appl. Polym. Sci.*, **25**, 597 (1980).
17. A. Takahara, K. Yamada, T. Kajiyama, and M. Takayanagi, *Rept. Progr. Polym. Phys., Jpn.*, **21**, 359 (1978).
18. M. Takayanagi, A. Takahara, K. Yamada, and T. Kajiyama, *Polym. Prepr., Am. Chem. Soc., Div. Polym. Chem.*, **20**(1), 263 (1979).
19. D. C. Prevorsek, Y. D. Kwon, R. K. Sharma, and E. T. Gilliam, U.S. Pat. 3,969,930, (1976).
20. D. C. Prevorsek, Y. D. Kwon, and R. K. Sharma, *J. Macromol. Sci. Phys., B*, **13**, 571 (1977).
21. D. C. Prevorsek, Y. D. Kwon, and R. K. Sharma, *Polym. Prepr., Am. Chem. Soc., Div. Polym. Chem.* **17**(2), 195 (1975).
22. A. Takahara, K. Yamada, T. Kajiyama, and M. Takayanagi, *Rept. Progr. Polym. Phys. Jpn.*, **23**, 383 (1980).
23. A. Takahara, K. Yamada, T. Kajiyama, and M. Takayanagi, *J. Mater. Sci.*, **15**, 2653 (1980).
24. A. Takahara, K. Yamada, T. Kajiyama, and M. Takayanagi, *Polym. Prepr., Jpn.*, **28**, 1762 (1979).
25. I. Constable, J. G. Williams, and D. J. Burns, *J. Mech. Eng. Sci.*, **12**, 20 (1970).
26. A. R. Payne, *J. Appl. Polym. Sci.*, **3**, 127 (1960).
27. T. R. Tauchert, *Int. J. Eng. Sci.*, **5**, 353 (1967).
28. T. R. Tauchert and S. M. Afzel, *J. Appl. Phys.*, **38**, 4568 (1967).
29. M. Takayanagi and T. Kajiyama, *J. Macromol. Sci., Phys., B*, **8**, 1 (1973).
30. M. A. Miner, *J. Appl. Mech., Trans. ASME*, **67**, A-127 (1949).
31. A. M. Freudenthal and R. A. Heller, *J. Aerospace Sci.*, **26**, 431 (1959).
32. D. C. Prevorsek and M. L. Brooks, *J. Appl. Polym. Sci.*, **11**, 925 (1967).

Received April 7, 1980
Accepted July 11, 1980